HHS Public Access

Author manuscript

Curr Opin Biotechnol. Author manuscript; available in PMC 2020 December 17.

Published in final edited form as:

Curr Opin Biotechnol. 2020 December ; 66: 78–87. doi:10.1016/j.copbio.2020.06.009.

Advances in microphysiological blood-brain barrier (BBB) models towards drug delivery

Caleb S Lee, **Kam W Leong**

Columbia University, NY, NY, 10027, United States

Abstract

Though the blood-brain barrier (BBB) is vital for the maintenance of brain homeostasis, it also accounts for a high attrition rate of therapies targeting the central nervous system (CNS). The challenge of delivery across the BBB is attributed to a combination of low permeability through an endothelium closely knit by tight and adherens junctions, extremely low rates of endothelial transcytosis, and efflux transporters. In the past decade, enormous research efforts have been spent to develop BBB penetration strategies using biochemical or physical stimuli, aided by BBB-on-chips or microphysiological BBB models to facilitate *in vitro* studies. Here, we discuss recent advances in BBB-chip technology that have enabled effective preclinical screenings of brain targeting therapeutics and external stimulation, such as sonoporation and electroporation, for improved BBB penetration.

Introduction

Comprising the brain and spinal cord, the CNS serves a crucial role in all physiological processes but are also prone to malfunction, leading to diseases including mental disorders (e.g. addiction, depression), neurodegenerative disorders (e.g. Alzheimer's, Huntington's, Parkinson's, motor neuron diseases), brain cancers (e.g. glioblastoma), and stroke. The annual economic burden of neurological and psychiatric malfunctions is roughly $800 billion in both the U.S. in 2014 and Europe in 2010, where Alzheimer's disease and other dementias add substantially to the cost [1,2]. The physical and financial toll is expected to grow with an aging population and a continuing rise in mental disorders. However, effective delivery of therapeutics to the brain remains a significant challenge.

Compared with the general difficulty of drug development to other tissues, CNS drugs face the additional challenge to penetrate the BBB, whereas most conventional preclinical tools lack the complexity and relevance to model the human BBB appropriately. *In vitro* models, such as parallel artificial membrane permeability assays (PAMPA) and cell-based Transwell assays, are well-suited for high-throughput screening but are oversimplified for physiological relevance [3]. *In vivo* animal models also lack clinical relevance, as significant

Corresponding author: Leong, Kam W (kam.leong@columbia.edu).

Conflict of interest statement

Nothing declared.

cross-species differences in barrier function markers–tight junctions (TJs), transporters, and receptors–between rodents and humans are found [4].

Recent advances in stem cell technology, microfluidics, and tissue engineering have led to the production of well-controlled micro-sized human tissues and organs that recapitulate the native microenvironment. These tissue-chip efforts can accelerate drug development by providing a platform for physiological pharmacokinetic modeling, thereby bridging the current gaps within *in vitro-in vivo* translation [5]. Other incentives of capturing human genetic, physiological, and pathological diversities in tissue-chips include the developments of (1) precision/personalized medicine via optimization of drug regimens to specific patient biology, (2) *in vitro* clinical trials for rare and pediatric diseases that are unfit for standard clinical trial designs, (3) and ethical replacements for animal studies [6]. In particular, this review explores several different BBB-chips, with emphasis on the accurate reproduction of drug transport pathways and the potential to perform effective preclinical screening of strategies designed to increase BBB penetration (Figure 1). Further, the BBB-chips are informally classified into 2D and 3D–not to be confused with 2D culture, which is usually on Transwell. As forerunners of microphysiological systems development, 2D tissue-chips are designed to effectively separate cell types and supply nutrients via diffusion from fluid flow. However, this separation is often too large and lacks an extracellular matrix (ECM) to mimic physiological cell-cell interactions. Instead, 3D BBB-chips aim to capture the defining features of brain microvasculature (e.g. circular cross-section, diameter, astrocytic endfeet) and generally contain natural basement membrane formed by cell-secreted ECM.

BBB physiology and drug delivery in the context of tissue chips

The BBB — human body's most formidable barrier — is built with tightly packed brain microvascular endothelial cells (BECs), pericytes embedded in the basement membrane, and astrocytic endfeet ensheathing the capillary (Figure 1). Contrary to the leaky peripheral vasculature, cerebrovasculature is held together by highly intricate TJs that block most small molecules (MW < 400 Da) and nearly all macromolecules from paracellular transport [7]. Efflux transporters–ATP-binding cassette (ABC) and some solute carrier (SLC) transporters–then act as extra barriers to pump out drugs back into the blood circulation (Figure 1).

The challenge of cerebral drug transport has become even more urgent with the shift in therapeutics from small-molecules to macro-molecules, such as antibody-drug conjugates and nanotherapeutics [8]. Despite these limitations, promising brain drug delivery routes exist, and capabilities of BBB-chips to assess these strategies can be confirmed with immunostaining and RT-qPCR of BBB functional markers–TJ proteins (e.g. ZO-1, occludins, claudins, junctional adhesion molecules), ABC transporters (e.g. P-gp, BCRP, MRP), and SLC transporters.

Trans-endothelial electrical resistance (TEER) offers a quantitative measure of TJ integrity, with the current gold standard of 1500–6000 Ω cm^2 measured in rats and frogs *in vivo* [3]. The consensus on the minimum required TEER for BBB-chips has not been established, but 500 and 900 Ω cm^2 for small and large molecules, respectively, are suggested based on

results from human induced pluripotent stem cell-derived BECs (hiBECs) [9]. However, as TEER measurement either requires custom-built electrodes or is incompatible with BBB-chip designs, the permeabilities of 3–70 kDa dextrans present a reasonable alternative (Figure 2). Considering that numerous chemotherapeutics do not fit in this range (e.g. doxorubicin, gemcitabine, paclitaxel), smaller particles should be more frequently tested, and comprehensive permeability studies using molecules of varying hydro-philicity will be beneficial. Many of these studies, including brain targeted nanomedicine, have already been done on Transwell settings and provide roadmaps to future screenings on BBB-chips [10].

BBB-chips

Two-dimensional modeling

Earliest BBB-chips are ‘evolved’ from the Transwell setup, by perpendicularly sandwiching a microporous semi-permeable membrane in between two microfabricated polymeric cell-culture compartments, referred to ‘brain’ and ‘blood’ sides (Figures 3a–c) [11••,12,13••,14–20]. Permeability can be easily assessed using fluorescent tracers, and TEER can be measured in real-time with custom-designed electrodes. Taking full advantage of hiBEC and its conditioning with hypoxia and retinoic acid, these BBB-chips can detect TEER > 4000 Ω cm^2 and lower permeability results than what is seen in rats *in vivo* (Figure 2) [11••,12,21]. Benefits of shear stress and co-culture (astrocytes with or without pericytes) to BEC have been demonstrated with comparative studies in numerous BBB-chips indicating improved barrier functions [11••,14,16,22–28].

Horizontally separating the two cellular compartments with microstructures, the parallel BBB-chips improve visualization and simplify the fabrication process by obviating the need for a membrane [22,23]. Using commercially available SynVivo, dextran permeabilities and interactions between BECs and astrocytes through the microstructures have been shown (Figure 3d) [23]. Another product OrganoPlate achieves the compartmental separation with ECM-gels and offers the high-throughput capability of 40 or 96 chips in a well-plate format (Figure 3e) [24].

In 2D BBB-chips, accurate representations of the BBB microenvironment are often limited by microfabrication (i.e. photolithography) and commercial microporous membranes. These microstructures (10–50 mm) separate BECs from astrocytes and pericytes in a few orders of magnitude farther than the basement membrane does *in vivo* (20–200 nm) [3]. Submicron ultrathin membranes offer close to physiological separation and can be beneficial at capturing high-resolution images of nanoparticle translocation and reducing background TEER [29]. Membrane structural (i.e. porosity, pore size, thickness) properties should also be carefully considered, as they impact cell–cell interactions and both diffusive and hydraulic permeabilities [30•]. Moreover, rectangular cross-sectional microchannels create an uneven shear stress distribution that can cause dysregulation of transcription factors that suppress the endothelial response to inflammatory stimuli [27,28,31].

Three-dimensional modeling

Emulating the circular cross-section of native vessels, tubular BBB-chips in the configuration of cylindrical microchannels can be formed by introducing microneedles or perfusion through an ECM-gel (Figure 3f–g) [25,26,32]. These BBB-chips achieve uniformly distributed flow profile and development of a natural basement membrane, as BECs secrete their own basal laminin [25,26]. The ‘lumens’ in tubular BBB-chips are still significantly larger (>100 μm) than those of brain capillaries (7–10 μm) or arterioles and venules (10–90 μm) [3].

Unlike the majority of BBB-chip approaches that engineer predetermined scaffolds on which microvessels can conform to, the vasculogenesis strategy aims to reconstruct the vasculature *de novo*. Once a cell-laden ECM gel is loaded into a microdevice, endothelial cells self-assemble into a vascular network, with pericytes and astrocytic endfeet directly attached to the surface (Figure 3h–i) [27,28,31,33•]. The self-assembled BBB-chips offer the closest mimicking of brain capillaries with hierarchical branching and ‘lumen’ diameter around 35 μm; however, due to the inherent heterogeneity in branching patterns, optimization is still required for reproducibility.

Organoid/spheroid platform is becoming increasingly relevant to and can advance synergistically with BBB-chip (Figure 3j–k) [34,35••,36,37]. Self-organized BBB cells formed under low-adhesion conditions, termed BBB organoids or spheroids, possess very high physiological relevance, as functional blood vessels are found in vascularized brain organoids implanted in mice [36]. Microfabrication techniques used in BBB-chips can help address some of the challenges of organoid/spheroid generation, such as nutrient supply, heterogeneity reduction, and spatiotemporal control of morphogenetic signaling pathway activation [38].

3D printing and bioprinting are promising techniques that can reduce the manufactural burden of the aforementioned modeling approaches and provide unprecedented structural controls. Two-photon lithography has been applied to fabricate a microfluidic system containing 50 parallel cylindrical and porous microcapillaries (10 μm diameter) (Figure 3l) [39]. Another group has recently developed a porous PCL/PLGA-based microfluidic vasculature network and measured TEER comparable (120 Ω cm^2) to that of other BBB-chips using immortalized murine lines (i.e. bEnd.3) (Figure 3m) [40].

Towards targeted drug delivery in BBB-chips

BBB disruption

For decades, mannitol has been clinically used as a hyperosmotic agent to reversibly open the BBB. Using BBB-chips, several groups have shown increased permeability of fluorescent particles following exposure to mannitol (Figure 4a) [11••,18,32]. In a constant mannitol concentration, the exposure duration dictates the permeability increase and reversibility [32].

Inflammation promoting substances are also widely known to disrupt the endothelial cell–cell junctions. Physiological response to histamine can be replicated in BBB-chips with

TEER drop and dextran permeability spike (Figure 4b) [14,17]. Similarly, an increased fluorescence is observed in the cores of histamine treated vascularized human cortex organoids [36]. Furthermore, vascular inflammatory cytokines TGF-β1, TNFα, IL-1β, and IL-8 increase permeability in BBB-chips [13••,19,26].

Cereport (RMP-7, bradykinin B2 agonist) is another inflammation modulator that has a potential clinical benefit. Co-administration of cereport and anti-cancer drugs show success in animal models but has not been translated clinically in glioma patients [41]. Further studies on doses, schedules, combination regimens, and conjugations with drug carriers may prove cereport useful and can be benefited from using BBB-chips.

Electroporation and sonoporation

Though effective at drug delivery, BBB disruption is seen in various diseases and can cause neuronal dysfunction, making its reversibility paramount for clinical applications. Thus recently, BBB disruption using external physical stimulations has drawn much attention as a non-invasive approach of spatiotemporally localized therapy. Using BBB-chips, the effect of electroporation has been reversed by tuning the parameters–frequency, amplitude, polarity, and duration–of high-magnitude pulsed electrical fields (Figure 4c) [18].

With its proven clinical utility in diagnostic imaging, the combined usage of ultrasound and microbubbles is particularly promising for safe and effective BBB disruption. Termed sonoporation, focused ultrasound (FUS) triggers microbubble cavitation and subsequent oscillation (stable cavitation) or collapse (inertial cavitation), leading to transient membrane permeabilization. The sonoporation effects are seen with increased intercellular junctional gap area, permeability, and cytotoxicity of doxorubicin-encapsulating liposomes in vascular-chips (Figure 4d) [42–45]. Vascular endothelial cells in these devices can be replaced with BECs for brain gene and drug delivery studies. Additional to the enhanced paracellular transport due to TJ disruption, heightened endocytosis is seen with stable cavitation [8]. Taking advantage of BBB-chips, operational parameters of insonation, microbubbles, and therapeutics concentration in conjunction with flow control can be optimized to further assess reversibility and establish the bioeffects of stable and inertial cavitations.

Adsorptive-mediated transport (AMT) and cell-penetrating peptides (CPPs)

Emerging evidence suggests that some cell-penetrating peptides (CPPs) can effectively cross the BBB. Though the exact mechanism of cellular entry varies depending on the CPP and remains controversial, it has been suggested that cationic CPPs take advantage of negatively charged BBB surface and adsorptive-mediated transport (AMT) [46]. Compared to the abundance of known CPPs, quantitative data on their BBB penetrability are still lacking.

Using BBB-chips, nanoparticle functionalization with gH625–a CPP derived from the herpes simplex virus 1–has enhanced BBB penetration for the first time (Figure 4e, top) [15]. In a more comprehensive study, a panel of 16 CPPs has been screened on vascularized human BBB spheroids, successfully predicting four candidates capable of crossing the mice BBB (Figure 4e, bottom) [35••].

Receptor-mediated transport (RMT)

Unlike AMT that suffers from the non-specific uptake, receptor-mediated transport (RMT) is highly specific, using receptors that are overexpressed on and can transport large proteins across the BBB. Anti-transferrin receptor (TfR) antibodies MEM75 and MEM189 have shown markedly higher penetration than those of control antibodies in BBB-chips [11••,24]. Taking a step further, transferrin conjugation has increased the permeabilities of polystyrene and polyurethane nanoparticles (Figure 4f) [33•].

LDLR-related protein-1 (LRP1), or apolipoprotein E receptor (ApoER), is another protein commonly targeted for RMT into the brain. Designed for LRP1 binding, angiopep-2 is a peptide ligand that has shown to increase brain penetration of conjugated drugs in numerous *in vitro* and *in vivo* models. ANG1005, a conjugate of angiopep-2 and chemotherapeutic paclitaxel, has had multiple successful phase II results and is expected to start phase III this year [41]. Thus, *in vitro* BBB penetration study using angiopep-2 is an effective method to validate RMT capability [35••]. BBB-chips can further examine the performance of surface-functionalized nanoparticles, as shown with angiopep-2 conjugated quantum dots and liposomes, and ApoE-conjugated SiO_2 nanoparticles (Figure 4g) [11••,16,29].

The scavenger receptor class B type 1 (SRB1) is one of the primary transport mechanisms of high-density lipoprotein (HDL) transcytosis into the brain. Using an HDL-mimetic nanoparticle, SRB1-mediated transcytosis has been validated in BBB-chips, as an SRB1 inhibitor (BLT1) substantially decreases BEC nanoparticle uptake [20].

Efflux transporter inhibition

Co-treatment with efflux inhibitors can potentially help a wide range of drugs to reach a therapeutic quantity in the brain. With successful modeling of efflux transporter functions, BBB-chips show increased permeation of various molecules following treatments with inhibitors of P-gp (verapamil, valspodar, and elacridar), MRP1 (MK571), and BCRP (elacridar and Ko143) (Figure 4h) [11••,28].

There are indications that riluzole, one of two approved drugs for amyotrophic lateral sclerosis (ALS), is a substrate of P-gp/BCRP and can improve ALS mice survival when used together with P-gp/BCRP inhibitor elacridar [47]. Similar combinatory studies using patient-specific BBB-chips can screen already approved drugs and provide more immediate translational benefits than some of the approaches discussed above.

Future perspectives

Although microphysiological systems development is still in the early stage, recent progress in BBB-chips has captured not only the essential biological functions but also the capability to screen targeted therapeutic approaches at an unprecedented level of physiological relevance *in vitro*. Optimization of cellular and microenvironment controls and standardization of barrier function quantification will help form a clinically relevant consensus across different types of BBB-chips.

For a BBB-chip to have an impact on drug development, the balance between accurate physiological representation and scalability is critical. Considering 3D printing approaches, two-photon lithography achieves a 1:1 scale of the brain microvasculature but may require cost-prohibitive infrastructure to mass-produce [39]. In contrast, simple extrusion-based printing of biocompatible polymer demonstrates a reasonable recapitulation with a low cost [40].

Advances in machine learning may also further reduce the cost of BBB-chip development. Incorporation of algorithms into data analysis can streamline cumbersome experimental design and improve reproducibility, as shown to benefit permeability measurements in self-assembled BBB-chips [33•].

Another apparent next step is the inclusion of biological fluids, such as serum and blood. Whole blood can add a plethora of new complications to already intricate models. However, the use of anticoagulants has eased this process, and an increasing number of groups are studying the blood-endothelium interface in microfluidic settings [48]. The benefits of using citrated whole blood in BBB-chips have been demonstrated by blood leakage through the endothelial layer only after TNF-a induction and by selective filtrations of immunoglobulin G, albumin, and transferrin [13••]. As peptide-nanocarrier and protein-nanocarrier conjugates are vulnerable to deactivation *in vivo* but much less so in culture medium, preclinical testing of targeted therapy and of blood-nano-therapeutic complications (chemical stability, colloidal stability, and protein corona formation) in blood or ‘blood substitutesc’ will have an enhanced physiological relevance and significant contribution to the development of next-generation CNS nanotherapeutics.

Acknowledgements

Funding support from N.I.H (UH3TR002151, UG3NS115598) and scientific discussions with Dr. Yang Xiao and Dr. Gad Vatine are gratefully acknowledged.

References and recommended reading

Papers of particular interest, published within the period of review, have been highlighted as

• of special interest

•• of outstanding interest

1. DiLuca M, Olesen J: The cost of brain diseases: a burden or a challenge? Neuron 2014, 82:1205–1208. [PubMed: 24945765]
2. Gooch CL, Pracht E, Borenstein AR: The burden of neurological disease in the United States: a summary report and call to action. Ann Neurol 2017, 81:479–484. [PubMed: 28198092]
3. DeStefano JG, Jamieson JJ, Linville RM, Searson PC: Benchmarking in vitro tissue-engineered blood–brain barrier models. Fluids Barriers CNS 2018, 15:32. [PubMed: 30514389]
4. Aday S, Cecchelli R, Hallier-Vanuxeem D, Dehouck MP, Ferreira L: Stem cell-based human blood–brain barrier models for drug discovery and delivery. Trends Biotechnol 2016, 34:382–393. [PubMed: 26838094]
5. Herland A, Maoz BM, Das D, Somayaji MR, Prantil-Baun R, Novak R, Cronce M, Huffstater T, Jeanty SSF, Ingram M et al.: Quantitative prediction of human pharmacokinetic responses to drugs via fluidically coupled vascularized organ chips. Nat Biomed Eng 2020, 4:421–436 10.1038/s41551-019-0498-9. [PubMed: 31988459]

6. Ronaldson-Bouchard K, Vunjak-Novakovic G: Organs-on-a-chip: a fast track for engineered human tissues in drug development. Cell Stem Cell 2018, 22:310–324. [PubMed: 29499151]

7. Tang W, Fan W, Lau J, Deng L, Shen Z, Chen X: Emerging blood–brain-barrier-crossing nanotechnology for brain cancer theranostics. Chem Soc Rev 2019, 48:2967–3014. [PubMed: 31089607]

8. Nowak M, Helgeson ME, Mitragotri S: Delivery of nanoparticles and macromolecules across the blood–brain barrier. Adv Ther 2020, 3:1900073.

9. Mantle JL, Min L, Lee KH: Minimum transendothelial electrical resistance thresholds for the study of small and large molecule drug transport in a human *in vitro* blood–brain barrier model. Mol Pharm 2016, 13:4191–4198. [PubMed: 27934481]

10. Aparicio-Blanco J, Martín-Sabroso C, Torres-Suárez A-I: In vitro screening of nanomedicines through the blood brain barrier: a critical review. Biomaterials 2016, 103:229–255. [PubMed: 27392291]

11••. Park TE, Mustafaoglu N, Herland A, Hasselkus R, Mannix R, FitzGerald EA, Prantil-Baun R, Watters A, Henry O, Benz M et al.: Hypoxia-enhanced blood-brain barrier chip recapitulates human barrier function and shuttling of drugs and antibodies. Nat Commun 2019, 10:2621. [PubMed: 31197168] An exemplary BBB-chip study for drug delivery with the highest reported TEER on chip and multiple delivery strategies, including BBB disruption, RMT and efflux inhibition. Benefits of hypoxic conditioning of hiBECs during differentiation was also highlighted.

12. Wang YI, Abaci HE, Shuler ML: Microfluidic blood–brain barrier model provides *in vivo*-like barrier properties for drug permeability screening. Biotechnol Bioeng 2017, 114:184–194. [PubMed: 27399645]

13••. Vatine GD, Barrile R, Workman MJ, Sances S, Barriga BK, Rahnama M, Barthakur S, Kasendra M, Lucchesi C, Kerns J et al.: Human iPSC-derived blood-brain barrier chips enable disease modeling and personalized medicine applications. Cell Stem Cell 2019, 24:995–1005. [PubMed: 31173718] This study showcases disease-modeling and personalized medicine capabilities of BBB-chips, by using three healthy donor iPSC lines and two patient-specific iPSC lines. MCT8-deficient patient-derived hiBECs showed reduced permeability of triiodothyronine and Huntington's disease patient-derived hiBECs exhibited higher dextran permeabilities than healthy hiBECs did. The MCT8 experiments were repeated using whole human blood and the overall permeability was reduced significantly.

14. Booth R, Kim H: Characterization of a microfluidic in vitro model of the blood-brain barrier (μBBB). Lab Chip 2012, 12:1784–1792. [PubMed: 22422217]

15. Falanga AP, Pitingolo G, Celentano M, Cosentino A, Melone P, Vecchione R, Guarnieri D, Netti PA: Shuttle-mediated nanoparticle transport across an *in vitro* brain endothelium under flow conditions. Biotechnol Bioeng 2017, 114:1087–1095. [PubMed: 27861732]

16. Papademetriou I, Vedula E, Charest J, Porter T: Effect of flow on targeting and penetration of angiopep-decorated nanoparticles in a microfluidic model blood-brain barrier. PLoS One 2018, 13:e0205158. [PubMed: 30300391]

17. Sato M, Sasaki N, Ato M, Hirakawa S, Sato K, Sato K: Microcirculation-on-a-chip: a microfluidic platform for assaying blood- and lymphatic-vessel permeability. PLoS One 2015, 10:e0137301. [PubMed: 26332321]

18. Bonakdar M, Graybill PM, Davalos RV: A microfluidic model of the blood-brain barrier to study permeabilization by pulsed electric fields. RSC Adv 2017, 7:42811–42818. [PubMed: 29308191]

19. Motallebnejad P, Thomas A, Swisher SL, Azarin SM: An isogenic hiPSC-derived BBB-on-a-chip. Biomicrofluidics 2019, 13:064119. [PubMed: 31768205]

20. Ahn SI, Sei YJ, Park HJ, Kim J, Ryu Y, Choi JJ, Sung HJ, MacDonald TJ, Levey AI, Kim YT: Microengineered human blood–brain barrier platform for understanding nanoparticle transport mechanisms. Nat Commun 2020, 11:175. [PubMed: 31924752]

21. Lippmann ES, Al-Ahmad A, Azarin SM, Palecek SP, Shusta EV: A retinoic acid-enhanced, multicellular human blood-brain barrier model derived from stem cell sources. Sci Rep 2014, 4:4160. [PubMed: 24561821]

22. Prabhakarpandian B, Shen M-C, Nichols JB, Mills IR, Sidoryk-Wegrzynowicz M, Aschner M, Pant K: SyM-BBB: a microfluidic Blood Brain Barrier model. Lab Chip 2013, 13:1093–1101. [PubMed: 23344641]

23. Deosarkar SP, Prabhakarpandian B, Wang B, Sheffield JB, Krynska B, Kiani MF: A novel dynamic neonatal blood-brain barrier on a chip. PLoS One 2015, 10:e0142725. [PubMed: 26555149]

24. Wevers NR, Kasi DG, Gray T, Wilschut KJ, Smith B, Vught R, Shimizu F, Sano Y, Kanda T, Marsh G et al.: A perfused human blood-brain barrier on-a-chip for high-throughput assessment of barrier function and antibody transport. Fluids Barriers CNS 2018, 15:23. [PubMed: 30165870]

25. Herland A, van der Meer AD, FitzGerald EA, Park T-E, Sleeboom JJF, Ingber DE: Distinct contributions of astrocytes and pericytes to neuroinflammation identified in a 3D human blood-brain barrier on a chip. PLoS One 2016, 11:e0150360. [PubMed: 26930059]

26. Partyka PP, Godsey GA, Galie JR, Kosciuk MC, Acharya NK, Nagele RG, Galie PA: Mechanical stress regulates transport in a compliant 3D model of the blood-brain barrier. Biomaterials 2017, 115:30–39. [PubMed: 27886553]

27. Campisi M, Shin Y, Osaki T, Hajal C, Chiono V, Kamm RD: 3D self-organized microvascular model of the human blood-brain barrier with endothelial cells, pericytes and astrocytes. Biomaterials 2018, 180:117–129. [PubMed: 30032046]

28. Lee S, Chung M, Lee S-R, Jeon NL: 3D brain angiogenesis model to reconstitute functional human blood-brain barrier *in vitro*. Biotechnol Bioeng 2019, 117:748–762. [PubMed: 31709508]

29. Hudecz D, Khire T, Chung HL, Adumeau L, Glavin D, Luke E, Nielsen MS, Dawson KA, McGrath JL, Yan Y: Ultrathin silicon membranes for in situ optical analysis of nanoparticle translocation across a human blood-brain barrier model. ACS Nano 2020, 14:1111–1122. [PubMed: 31914314]

30•. Chung HH, Mireles M, Kwarta BJ, Gaborski TR: Use of porous membranes in tissue barrier and co-culture models. Lab Chip 2018, 18:1671–1689. [PubMed: 29845145] A comprehensive review of considerations for porous membranes in tissue chips, detailing the differences in mechanical, surface, and optical properties and the impact of pore size on cell-cell interactions. Membrane's impacts on permeability and TEER are also reviewed.

31. Phan DT, Bender RHF, Andrejecsk JW, Sobrino A, Hachey SJ, George SC, Hughes CC: Blood–brain barrier-on-a-chip: microphysiological systems that capture the complexity of the blood–central nervous system interface. Exp Biol Med 2017, 242:1669–1678.

32. Kim JA, Kim HN, Im SK, Chung S, Kang JY, Choi N: Collagen-based brain microvasculature model *in vitro* using three-dimensional printed template. Biomicrofluidics 2015, 9:024115. [PubMed: 25945141]

33•. Lee SWL, Campisi M, Osaki T, Possenti L, Mattu C, Adriani G, Kamm RD, Chiono V: Modeling nanocarrier transport across a 3D In vitro human blood-brain-barrier microvasculature. Adv Healthc Mater 2020:e190148610.1002/adhm.201901486. [PubMed: 32125776] This study illustrates how self-assembled BBB-chips, which is a less common but exceptionally physiologically relevant approach, can be applied to screen brain-penetrating nanoparticles.

34. Bergmann S, Lawler SE, Qu Y, Fadzen CM, Wolfe JM, Regan MS, Pentelute BL, Agar NYR, Cho CF: Blood–brain-barrier organoids for investigating the permeability of CNS therapeutics. Nat Protoc 2018, 13:2827–2843. [PubMed: 30382243]

35••. Cho CF, Wolfe JM, Fadzen CM, Calligaris D, Hornburg K, Chiocca EA, Agar NYR, Pentelute BL, Lawler SE: Blood-brain-barrier spheroids as an in vitro screening platform for brain-penetrating agents. Nat Commun 2017, 8:15623. [PubMed: 28585535] The study effectively demonstrates BBB organoids/spheroids can be applied for high-throughput screening of brain-penetrating agents using 16 known and unknown CPPs for brain-penetrability.

36. Cakir B, Xiang Y, Tanaka Y, Kural MH, Parent M, Kang YJ, Chapeton K, Patterson B, Yuan Y, He CS et al.: Engineering of human brain organoids with a functional vascular-like system. Nat Methods 2019, 16:1169–1175. [PubMed: 31591580]

37. Nzou G, Wicks RT, Wicks EE, Seale SA, Sane CH, Chen A, Murphy SV, Jackson JD, Atala AJ: Human cortex spheroid with a functional blood brain barrier for high-throughput neurotoxicity screening and disease modeling. Sci Rep 2018, 8:7413. [PubMed: 29743549]

38. Park SE, Georgescu A, Huh D: Organoids-on-a-chip. Science 2019, 364:960–965. [PubMed: 31171693]
39. Marino A, Tricinci O, Battaglini M, Filippeschi C, Mattoli V, Sinibaldi E, Ciofani G: A 3D real-scale, biomimetic, and biohybrid model of the blood-brain barrier fabricated through two-photon lithography. Small 2018, 14:1702959.
40. Yue H, Xie K, Ji X, Xu B, Wang C, Shi P: Vascularized neural constructs for ex-vivo reconstitution of blood-brain barrier function. Biomaterials 2020, 245:119980. [PubMed: 32229330]
41. Dong X: Current strategies for brain drug delivery. Theranostics 2018, 8:1481–1493. [PubMed: 29556336]
42. Park YC, Zhang C, Kim S, Mohamedi G, Beigie C, Nagy JO, Holt RG, Cleveland RO, Jeon NL, Wong JY: Microvessels-on-a-chip to assess targeted ultrasound-assisted drug delivery. ACS Appl Mater Interfaces 2016, 8:31541–31549. [PubMed: 27781429]
43. DeOre BJ, Galie PA, Sehgal CM: Fluid flow rate dictates the efficacy of low-intensity anti-vascular ultrasound therapy in a microfluidic model. Microcirculation 2019, 26:e12576. [PubMed: 31140665]
44. Silvani G, Scognamiglio C, Caprini D, Marino L, Chinappi M, Sinibaldi G, Peruzzi G, Kiani MF, Casciola CM: Reversible Cavitation-induced junctional opening in an artificial endothelial layer. Small 2019, 15:e1905375. [PubMed: 31762158]
45. Juang EK, De Cock I, Keravnou C, Gallagher MK, Keller SB, Zheng Y, Averkiou M: Engineered 3D microvascular networks for the study of ultrasound-microbubble-mediated drug delivery. Langmuir 2019, 35:10128–10138. [PubMed: 30540481]
46. Guidotti G, Brambilla L, Rossi D: Cell-penetrating peptides: from basic research to clinics. Trends Pharmacol Sci 2017, 38:406–424. [PubMed: 28209404]
47. Jablonski MR, Markandaiah SS, Jacob D, Meng NJ, Li K, Gennaro V, Lepore AC, Trotti D, Pasinelli P: Inhibiting drug efflux transporters improves efficacy of ALS therapeutics. Ann Clin Transl Neurol 2014, 1:996–1005. [PubMed: 25574474]
48. Hesh CA, Qiu Y, Lam WA: Vascularized microfluidics and the blood-endothelium interface. Micromachines-basel 2019, 11:18.
49. Yuan W, Lv Y, Zeng M, Fu BM: Non-invasive measurement of solute permeability of rat pial microvessels. Northeast Bioengin C 2007 10.1109/nebc.2007.4413340.
50. Shi L, Zeng M, Sun Y, Fu BM: Quantification of blood-brain barrier solute permeability and brain transport by multiphoton microscopy. J Biomech Eng 2014, 136:031005. [PubMed: 24193698]

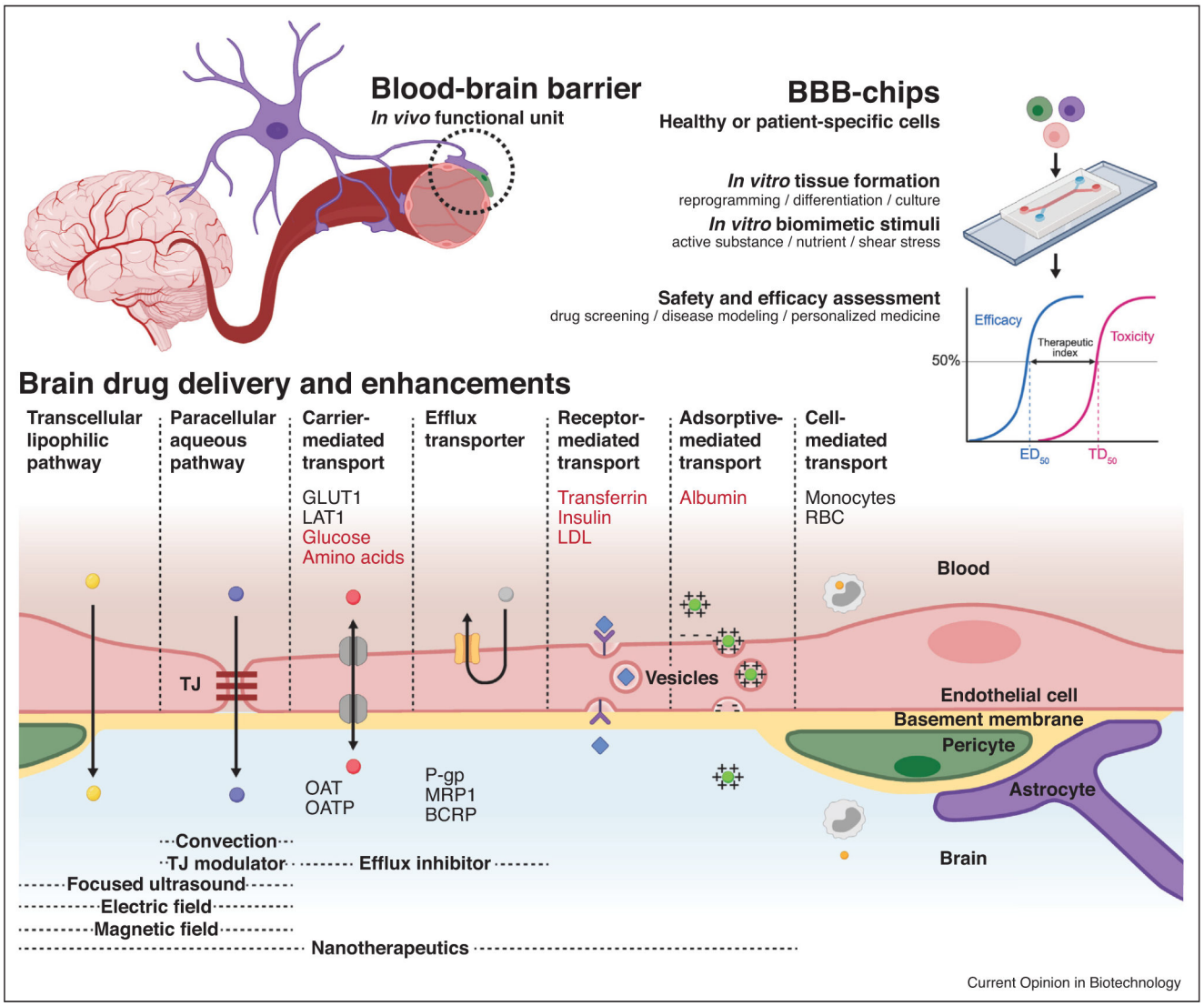

Figure 1.

Rationale for development of BBB-chips. BBB-chips can culture cells and apply controlled stimuli that are biomimetic of the human BBB's functional unit, allowing preclinical assessment of drug candidate safety and efficacy. Playing a critical role in the BBB, TJs are composed of membrane proteins anchored to and strengthened by networks like zonula occludens-1 (ZO-1), forming a tremendous barrier. Still, researchers have been able to deliver drugs to the brain using transcellular lipophilic pathway, paracellular aqueous pathway, and transports mediated by solute carriers (SLC), receptors, adsorptives, and cells [7,8]. Biological molecules that can cross the BBB are shown in red and are widely studied as surface functionalization motifs for brain targeting nanotherapeutics. Main biological components involved in the brain penetration–glucose transporter 1 (GLUT1), large neutral amino acid transporter (LAT1), monocytes, and red blood cells (RBCs)–are indicated on the blood side. Inversely, efflux transporters of both the SLC and ATP-binding cassette (ABC) superfamilies are listed on the brain side of the illustration. Organic anion transporters (OATs/SLC22A), organic anion transporting polypeptides (OATPs/SLCO), P-glycoprotein

(P-gp/ABCB1), breast cancer resistance protein (BCRP/ABCG2), and multidrug resistance protein 1 (MRP1/ABCC1) are some of these efflux transporters that can be inhibited to facilitate brain drug delivery. Further biochemical and physical enhancements can be achieved using TJ modulators, convection, focused ultrasound, electrical field, and magnetic field. Growing numbers of BBB-chip studies involve these pathways and enhancements to assess targeted drug delivery to the brain. Partially created with BioRender.com.

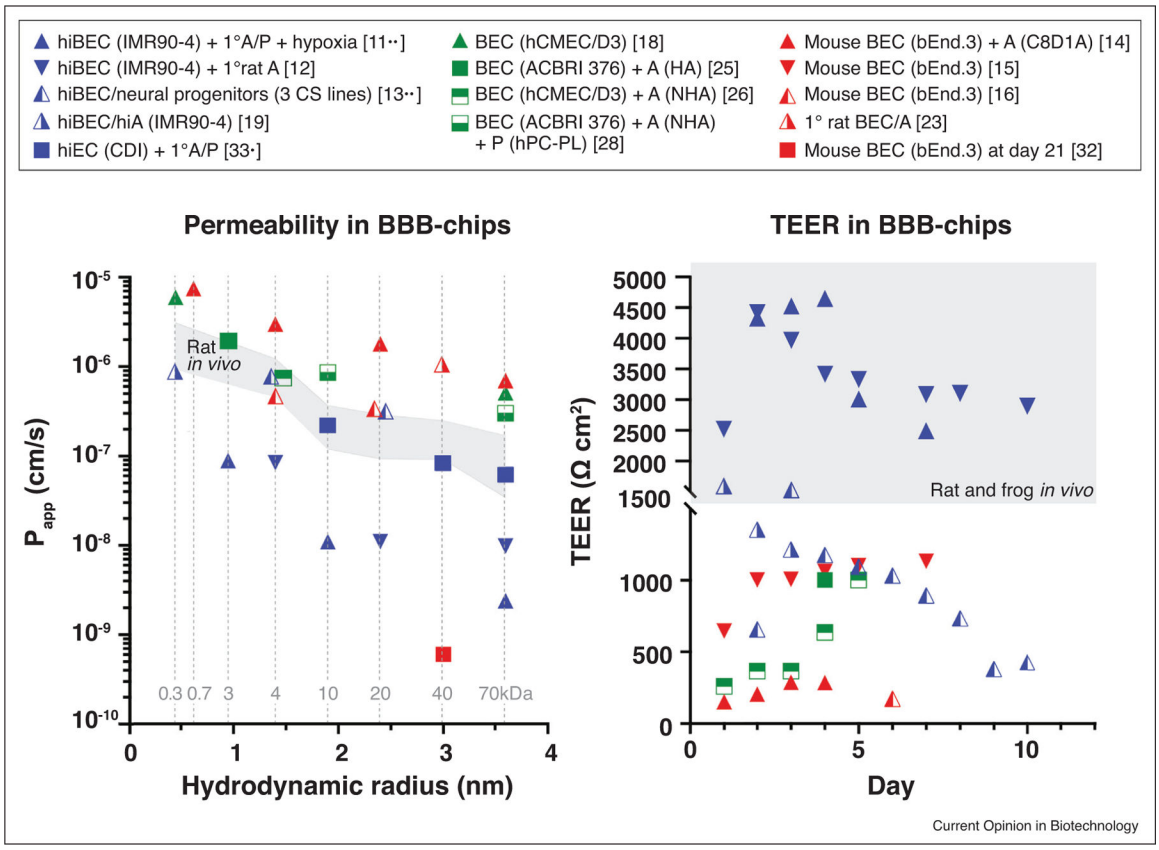

Figure 2.

Comparisons of barrier function in various BBB-chips. The results from two *in vivo* rat reports–routinely cited as gold standards of apparent permeability–mark the shaded range [49,50]. Fluorescent tracers used in these studies are denoted with gray dotted lines, with 332 Da sodium fluorescein, 668 Da propidium iodide, and 3–70 kDa dextrans. Human iPSC-derived BECs (hiBECs) show the lowest permeabilities and the highest TEER, with the exception of murine BECs long term culture (21 days) in a tubular BBB-chip [11••,12,13••,14–16,18,19,23,25,26,28,32,33•]. Triangle: 2D BBB-chip, square: 3D BBB-chip, blue: hiPSC-derived, green: human, orange: murine, 1°: primary, A: astrocytes, P: pericytes, CS: Cedars-Sinai.

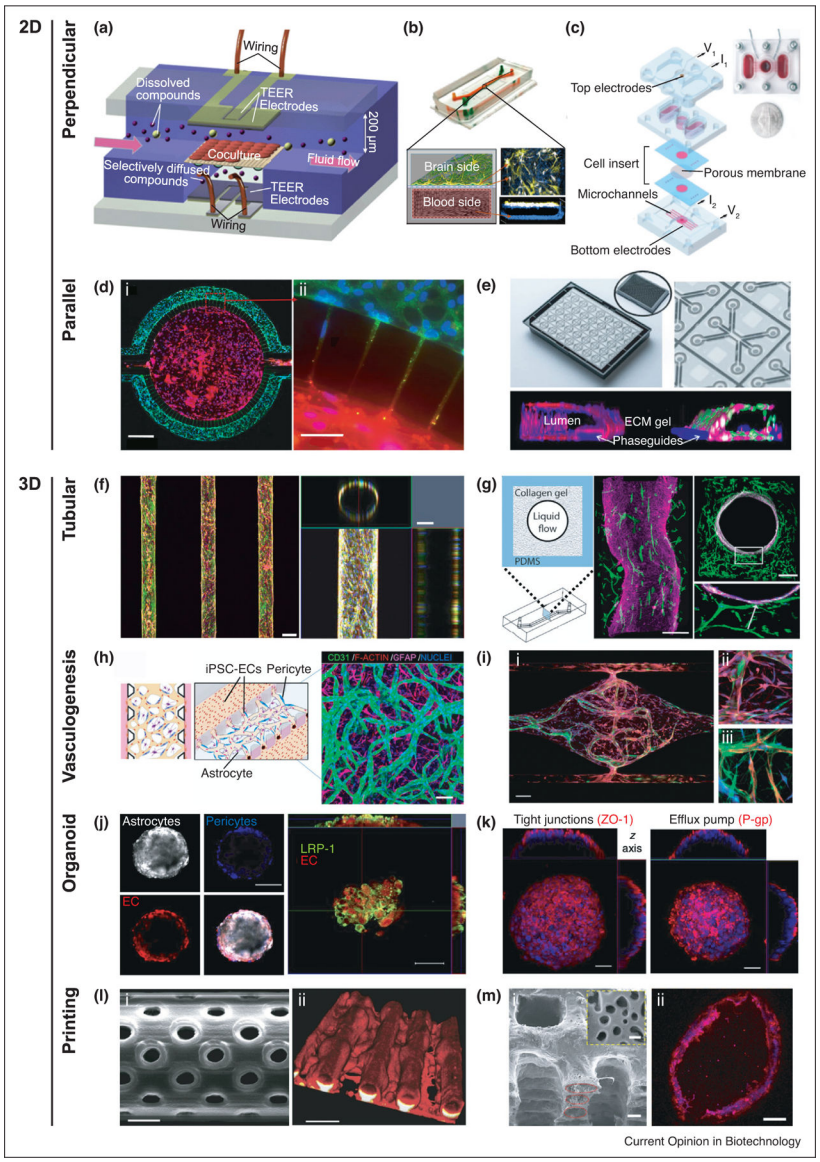

Figure 3.

Emerging technologies of *in vitro* BBB modeling. **(a)** Schematic of two perpendicular flow channels and TEER electrodes on the opposite ends [14]. **(b)** Microfluidic BBB-chip with hiBEC cultured on all surfaces of the basal ‘blood side’ and primary human brain astrocytes and pericytes on the upper surface of the semi-permeable membrane in the apical ‘brain side’ [11••]. **(c)** Exploded view of a platform, consisting of a cell-insert and three 3D printed plastic layers–bottom perfusion layer, middle reservoir and neuronal chamber layer, and top electrodes layer [12]. **(d)** (i) Parallel separation of BEC and astrocytes in a BBB-chip with (ii) cell–cell interactions through the microstructure [23]. **(e)** BBB co-culture in the three-lane OrganoPlate containing 40 chips. Collagen-I gel in the mid-lane separates lumen in the left lane from astrocytes and pericytes in the right lane [24]. **(f)** Confocal fluorescence micrographs showing a top view of the microvasculature array and an orthogonal view of the cylindrical lumen [32]. Microneedles are used to create cylindrical structures inside a

collagen gel. **(g)** Schematic of the pressure-driven viscous fingering method and resulting fluorescence confocal micrographs of endothelium surrounded by astrocytes [25]. **(h)** Schematic and confocal image of a self-assembled BBB microvascular network [27]. **(i)** (i) Immunostaining of self-assembled microvascular network formed by endothelial cells and astrocytes [31]. (ii) Astrocytic endfeet (red) directly interacting with the vessel (green). (iii) Pericytes (green) wrapping around the vessel (red) and interacting with astrocytes (blue). **(j)** Confocal images showing the organization of human astrocytes, pericytes, and BEC when co-cultured to form a spheroid. LRP1 expression is also shown [35••]. **(k)** TJ marker and P-gp efflux pump on the BBB organoid surface [34]. **(l)** (i) Scanning electron micrograph of a cylindrical microchannel with 1 μm diameter pores made using two-photon lithography [39]. (ii) F-actin staining of bEnd.3 cells. **(m)** (i) Scanning electron micrograph depicting layers of PCL/PLGA tubal network, which are molded from a 3D printed sacrificial template [40]. The yellow dashed inset displays the micropores on the channel wall. (ii) Cross-sectional image of the endothelialized channel.

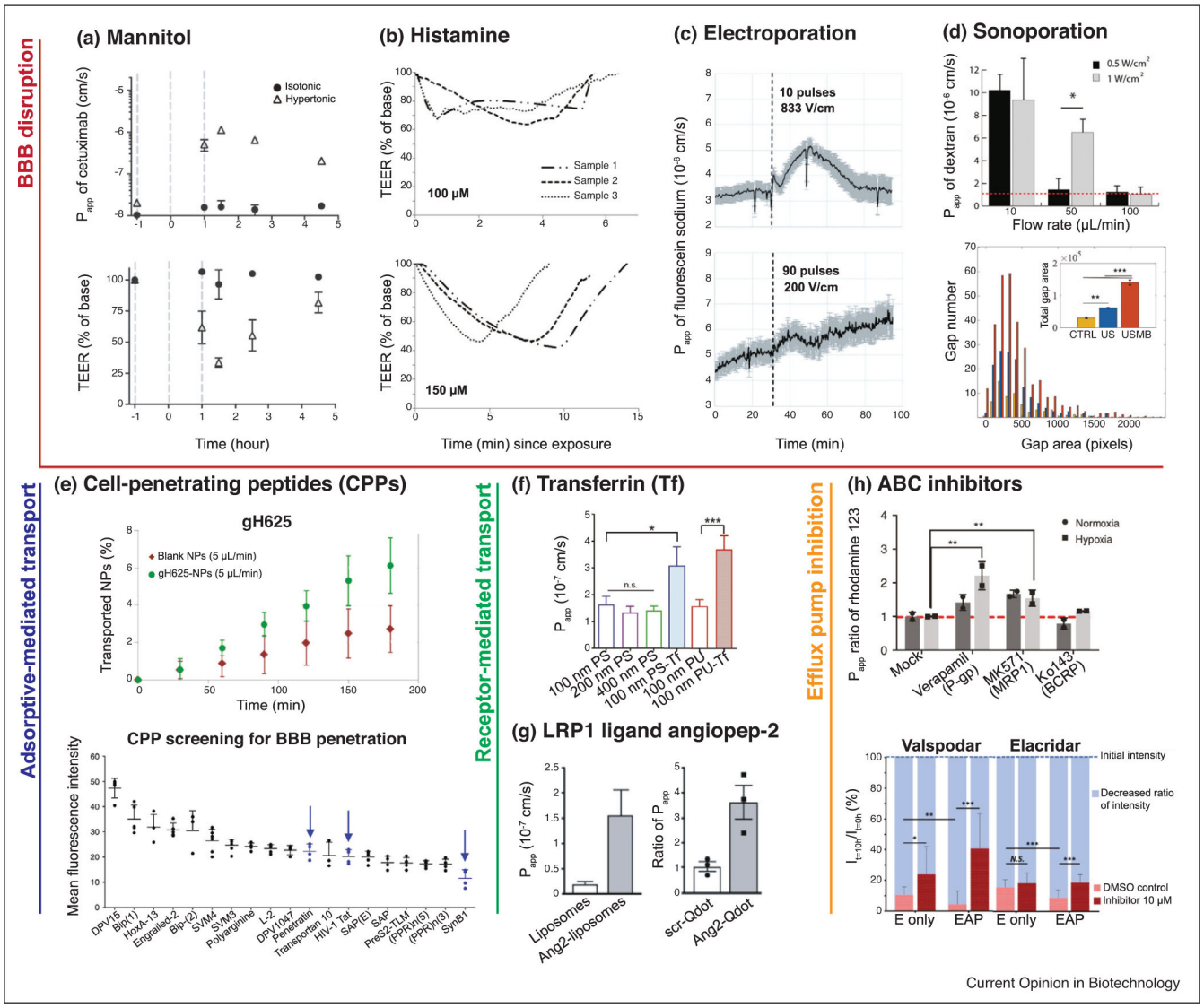

Figure 4.

Drug delivery strategies in BBB-chips. **(a)** BBB disruption after hyperosmolar mannitol treatment shown with cetuximab permeability spike and TEER drop [11••]. **(b)** Continuous TEER responses to two doses of histamine exposure [14]. Barrier functions recover within 6 and 15 μin after 100 and 150 mM exposures, respectively. **(c)** Enhanced permeabilization of fluorescent sodium salt after electroporation via 10 pulses of 833 V/cm (reversible) and 90 pulses of 200 V/cm (irreversible) [18]. The dashed line indicates pulse application. (**d**, top) Sonoporation in vascular-chips demonstrates vessel permeability changes due to varying levels of ultrasound intensity and microbubble perfusion rates [43]. Red dashed line indicates the control. (d, bottom) Junctional opening comparison of untreated (CTRL), ultrasound irradiated (US), and microbubble injected ultrasound irradiated (USMB) samples [44]. (**e**, top) Improved transport of 100 nm polystyrene (PS) nanoparticles (NPs) after surface functionalization with gH625 [15]. (e, bottom) 16 CPPs tested for brain penetration using BBB spheroids [35••]. Well-established BBB-penetrating CPPs are pointed out with

arrows. **(f)** Higher apparent permeabilities of PS and polyurethane (PU) NPs when transferrin (Tf) is conjugated [33•]. **(g)** Shuttling effects of angiopep-2-conjugation on liposomal and quantum dot NPs [11••,16]. (**h**, top) Inhibition of efflux transporters P-gp and MRP1 shown with the increased permeabilities of their substrate rhodamine 123 [11••]. Similar trends appear with P-gp substrate doxorubicin and P-gp/BCRP substrate DiOC2, which are not replicated here. The benefit of hypoxia-conditioned hiBEC differentiation is also highlighted. (h, bottom) P-gp inhibition using valspodar and elacridar. The decreases in calcein-AM fluorescence from initial levels are calculated to compare the efflux rates. The effect of elacridar is seen in triculture (EAP) but not in monoculture (E only) [28].